

MIT Open Access Articles

*Playing with Puffball: Simple Scale-Invariant
Inflation for Use in Vision and Graphics*

The MIT Faculty has made this article openly available. **Please share** how this access benefits you. Your story matters.

Citation: Nathaniel R. Twarog, Marshall F. Tappen, and Edward H. Adelson. 2012. Playing with Puffball: simple scale-invariant inflation for use in vision and graphics. In Proceedings of the ACM Symposium on Applied Perception (SAP '12). ACM, New York, NY, USA, 47-54.

As Published: <http://dx.doi.org/10.1145/2338676.2338686>

Publisher: Association for Computing Machinery (ACM)

Persistent URL: <http://hdl.handle.net/1721.1/95489>

Version: Author's final manuscript: final author's manuscript post peer review, without publisher's formatting or copy editing

Terms of use: Creative Commons Attribution-Noncommercial-Share Alike



Playing with Puffball: Simple scale invariant inflation for use in vision and graphics

Nathaniel R. Twarog*
MIT

Marshall F. Tappen†
University of Central Florida

Edward H. Adelson‡
MIT

Abstract

We describe how inflation, the act of mapping a 2D silhouette to a 3D region, can be applied in two disparate problems to offer insight and improvement: silhouette part segmentation and image-based material transfer. To demonstrate this, we introduce Puffball, a novel inflation technique, which achieves similar results to existing inflation approaches – including smoothness, robustness, and scale and shift-invariance – through an exceedingly simple and accessible formulation. The part segmentation algorithm avoids many of the pitfalls of previous approaches by finding part boundaries on a canonical 3-D shape rather than in the contour of the 2-D shape; the algorithm gives reliable and intuitive boundaries, even in cases where traditional approaches like the Minima rule are misled. To demonstrate its effectiveness, we present data in which subjects prefer Puffball’s segmentations to more traditional Minima-rule-based segmentations across several categories of silhouettes. The texture transfer algorithm utilizes Puffball’s estimated shape information to produce visually pleasing and realistically synthesized surface textures with no explicit knowledge of either underlying shape.

Keywords: object recognition, texture, lighting, shading and textures

Links: [DL](#) [PDF](#)

1 Introduction

Mapping a two-dimensional silhouette to a three-dimensional region – a task referred to as inflation – has been widely used in the design of sketch interfaces, such as the Teddy system, to create a smooth three-dimensional shape from a sketched outline [Alexe et al. 2004; Igarishi et al. 1999; Karpenko et al. 2002; Tai et al. 2004]; it has also been integrated with user input in systems tackling the problem of single-view reconstruction [Oswald et al. 2009; Prasad et al. 2006; Terzopoulos et al. 1987; Terzopoulos and Witkin 1988; Zhang et al. 2002]. Beyond these applications, inflation offers a convenient way to move between the two-dimensional and three-dimensional domains, and the results can often be intuitive as humans already comprehend a strong relationship between silhouettes and three-dimensional shapes [Tse 2002].

*e-mail:ntwarog@mit.edu

†e-mail:mtappen@cs.ucf.edu

‡e-mail:adelson@csail.mit.edu

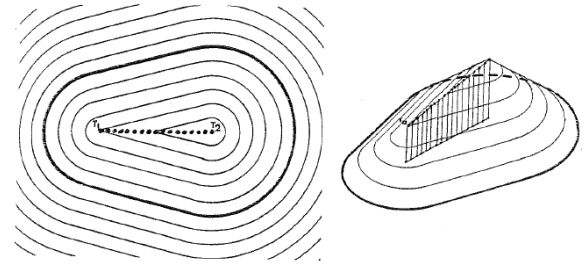


Figure 1: *The grassfire height function. Iteratively eroding the contour of the shape yields a sequence of smaller shapes. The sum of these shapes is the grassfire height function. The ridge along the top of this function marks the medial axis of the shape.*

The grassfire height function, proposed by Blum [1967], can be thought of as a simple form of inflation. The silhouette is repeatedly eroded, resulting in a sequence of smaller and smaller silhouettes; these silhouettes can be summed over time to yield a height function on the interior points of the original silhouette, where the height at a point is equal to the distance to the nearest edge (see Figure 1). Blum, of course, was not solving the problem of inflation, but rather calculating the medial axis transform, or MAT, in an effort to create a perceptually relevant skeletal shape descriptor.

The grassfire function forms the basis of many popular methods of creating beveled shapes in images, such as the Bevel and Emboss operation in Adobe Photoshop. A silhouette, such as the pair of Bs in Figure 2a, is passed through the grassfire function to give a beveled three-dimensional shape (Figure 2b). This shape can then be passed through a point-nonlinearity to give an appealing, rounded shape; but the result is scale-dependent, so the inflation of the smaller B is not simply a scaled-down version of the larger B (Figure 2c). The two Bs can be scaled properly if they are passed through different point non-linearities (Figure 2d), but in many situations a more desirable inflation approach is one which is inherently scale-invariant, and doesn’t depend on post-hoc normalizations. Some existing approaches to inflation, including that used in the Teddy system, achieve this inherent scale-invariance.

In this paper, we discuss two open problems where an intuitive, scale-invariant inflation tool can offer insight. The first is segmentation of two-dimensional silhouettes into parts; the second is image-based material transfer, which we accomplish as a pseudo-shape-based texture transfer. We also introduce a new method for scale-invariant silhouette inflation, which we call Puffball. It is important to note that many existing inflation techniques, though powerful, require a carefully crafted mix of computational, empirical and heuristic tools to function as desired. Puffball, on the other hand, has the advantage of being extremely simple to define and implement, making it an ideal candidate as a general-purpose inflation tool. We will formally define Puffball, and then describe the role of inflation in these two applications and explain how Puffball is applied to these problems in detail.

The results we describe for these two applications are not uniquely dependent on Puffball; any sufficiently intuitive scale-invariant in-

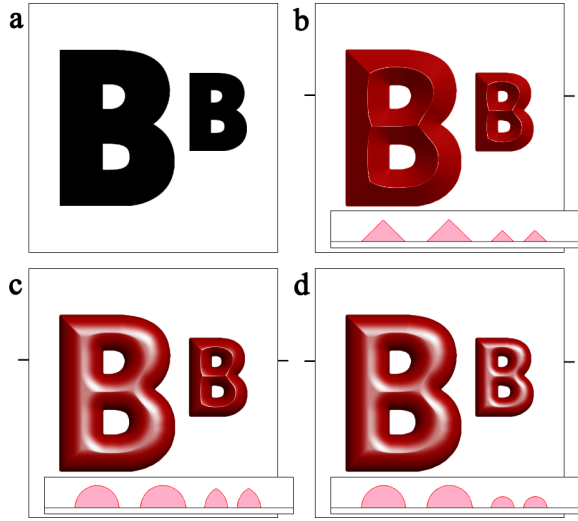


Figure 2: A bevel-inspired inflation approach. (a) Two similar B silhouettes. (b) The grassfire height function of silhouette 2a. A cross-section of the height function at the level marked by the hashes is shown in the inset. (c) Passing the grassfire height function through a non-linearity can yield a circular cross-section in one shape, but not both shapes simultaneously. (d) To get scale-invariance, the two B s must be passed through different point nonlinearities.

flation technique will work equally well. However, we have used Puffball inflation for both problems, because of its straightforward definition and ease of implementation.

2 Definition of Puffball Inflation

At the core of Puffball inflation is the principle: *anywhere you can place a circle, place a sphere*. In fact, this principle can fully describe the output of Puffball inflation; in equation form, the Puffball inflation I of a silhouette S can be written:

$$I(S) = \bigcup \{B^3(p, r) \mid B^2(p, r) \subset S\} \quad (1)$$

where $B^3(p, r)$ is the spherical ball centered on point p with radius r , and $B^2(p, r)$ is the circular region centered on p with radius r contained in the plane of S . The set of such circles, however, is massive: at any interior point of S , infinitely many circles centered on that point lie entirely within S . Thus Equation 1 is an elegant but impractical approach to silhouette inflation. Fortunately, the process can be greatly accelerated by noting that

$$B^2(p_1, r_1) \subset B^2(p_2, r_2) \Rightarrow B^3(p_1, r_1) \subset B^3(p_2, r_2)$$

So, in calculating the Puffball volume, we need only consider those circles not contained in any larger circle which is also contained in S ; that is, we need only consider the maximal circles of S . The centers and radii of the maximal circles of a silhouette S form the medial axis transform, or MAT, of the silhouette. As mentioned above, the MAT can be calculated by locating the ridges of the grassfire height function; this leads us to an alternative – and much more practical – definition of Puffball inflation:

$$I(S) = \bigcup \{B^3(p, r) \mid (p, r) \in \text{MAT}(S)\} \quad (2)$$

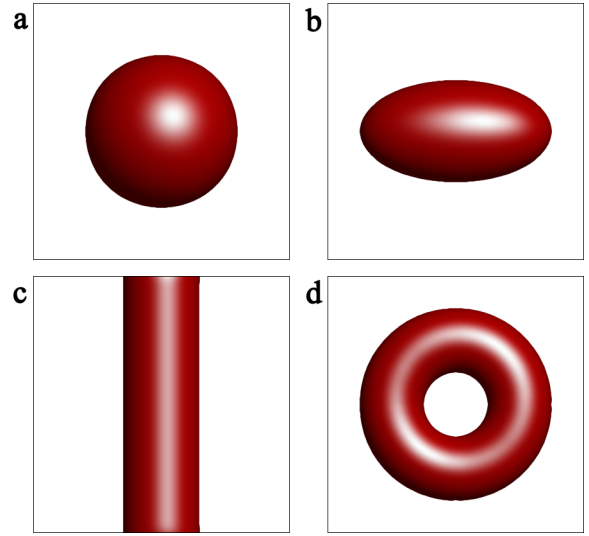


Figure 3: Output of Puffball inflation for several simple shapes.

Box 1 contains the MATLAB code implementing the algorithm; our implementation takes a binary image as input and gives a height map image as output. Note that we do not calculate the union of spheres by simply taking the maximum; instead we use a soft maximum achieved by adding the exponential of each of the component spheres, and then taking a logarithm of the resulting sum. If a raw maximum is used, small numerical errors in the calculation of the grassfire height function (unavoidable in a discrete image) result in unsightly and perceptually inconsistent creases; the soft maximum eliminates these creases, while having a negligible effect on the overall shape of the output.

Our discrete implementation of Puffball contains only one parameter, a scale parameter implicit in the soft-max technique; the continuous definition of Puffball in equation 2 has no parameters whatsoever. For the remainder of this paper, we have used Puffball as implemented in Box 1, with no parameter changes of any kind, so its behavior is as intuitive as possible. Fortunately, we have found

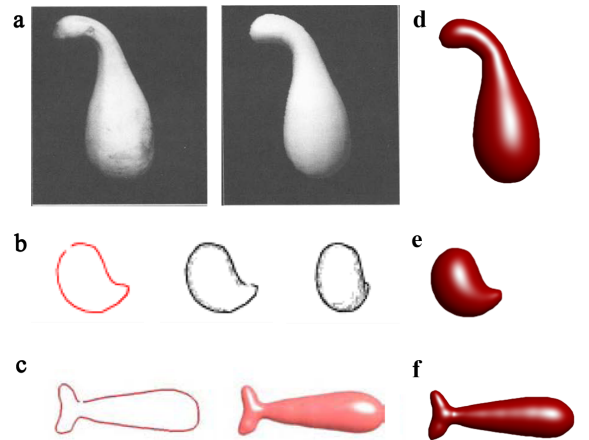


Figure 4: (a,b,c) Results of published inflation techniques, from (a) Terzopoulos et al. [1987], (b) Igarishi et al. [2001], and (c) Alexe et al. [2004]. (d,e,f) Results of Puffball inflation on the same inputs. All three results are successfully replicated.

```

function h = Puffball(mask)
    % CALCULATE GRASSFIRE HEIGHT FUNCTION %
    % A 3x3-tap filter to smoothly erode an anti-aliased edge
    fil = [0.1218 0.4123 0.1218; 0.4123 0.9750 0.4123; ...
          0.1218 0.4123 0.1218]/1.2404;
    nmask = double(mask);
    surf = zeros(size(mask));
    while ~isempty(find(nmask,1))
        surf = surf+nmask/1.67; % Each iteration erodes the edge .6 pixels
        nmaskpad = padarray(nmask,[1 1],'replicate');
        nmaskpad = conv2(nmaskpad,fil,'same')-1.4241;
        nmask = max(min(nmaskpad(2:end-1,2:end-1),1),0);
    end

    % LOCATE THE MEDIAL AXIS %
    [dx dy] = gradient(surf);
    dsurf = sqrt(dx.^2+dy.^2);
    % Medial axis points have a grassfire gradient measurably less than 1
    matr = bwmorph(dsurf<0.958&surf>2,'skel',Inf).*surf;

    % TAKE THE UNION (SOFT-MAX) OF MAXIMAL SPHERES %
    [X Y] = meshgrid(1:size(mask,2),1:size(mask,1));
    h = ones(size(mask));
    [y x] = find(matr);
    for i = 1:length(f)
        r = matr(y(i),x(i))^2 - (X-y(i)).^2 - (Y-x(i)).^2;
        h(r>0) = h(r>0)+exp(sqrt(r(r>0)));
    end
    h = log(h);
end

```

Box 1: MATLAB code implementing Puffball inflation.

Puffball works extremely well as it is, right “out of the box.”

As Figure 3 shows, Puffball performs intuitively on a wide range of simple inputs: a circle maps to a sphere, an ellipse maps to a prolate ellipsoid, etc. Figure 4 shows inflation results from several published inflation techniques. Terzopoulos et al. [1987; 1988] perform their inflation by wrapping a virtual elastic sheet around a user-provided axis, which is then iteratively deformed to match the bounding contour of the given silhouette. Igarishi et al. [1999] propose building an inflation around central axis structure similar to the medial axis; the shape is constructed by stitching together semicircular ribs built out from this central axis. Alexe et al. [2004] build on that work by using the same central axis structure to define a carefully optimized sum of spherical potential functions on 3D space, the level surface of which yields an intuitive inflation. Despite the disparate nature of these approaches, and the differences in their stated goals (Terzopoulos et al. [1987; 1988] hoped to model veridical 3D shape perception and reconstruction, while Igarishi et al [1999] and Alexe et al. [2004] proposed their methods as shape-sketching tools), as the figure shows, Puffball successfully replicates all three results. Puffball is inherently scale invariant, as shown in Figures 5a and 5b. Puffball can also take inputs of arbitrary complexity and topology; Figures 5c and 5d show the results on an arbitrary silhouette generated by thresholding random low-pass noise. For physically-inspired inflation approaches, such as those using deformable surfaces [Karpenko and Hughes 2006; Pentland 1990; Terzopoulos et al. 1987; Terzopoulos and Witkin 1988], this image would require considerable pre-processing, as the surface to be optimized must have the same topology as the final output. No such processing is required for Puffball.

It is also worth noting that Puffball is unique among inflation approaches as it makes no use of traditional 3D representation tools like triangle or polygonal meshes; every operation of Puffball’s im-

plementation occurs in the image domain, a fact which makes it much easier to understand and implement and sets it apart from the existing inflation literature. A triangle mesh could of course be derived from the height map output by Puffball, but we have found in the applications that follow that operating in the image domain is often far simpler.

We do not claim that Puffball is the last word in inflation, or a fully accurate model of human intuition about the relationship between 2D and 3D shape. For example, note how in Figure 5d, the shape contains noticeable bulges and creases. These are not the result of improper setting of the implicit soft-max parameter, but inherent effects of Puffball inflation. In addition, while most human observers interpret symmetric contours as bounding surfaces of revolution, Puffball make no such prediction. These limitations could almost certainly be overcome by increasing the flexibility and sophistication of the underlying algorithm. But for us, Puffball’s greatest strength has been its simplicity, so we have tried to investigate its potential as it is, with no optimizations or added complexity.

3 Applications of Inflation

3.1 Silhouette Part Segmentation

Parsing silhouettes into parts is a classic vision problem. Hoffman and Richards [1987] propose an approach to silhouette part segmentation utilizing minima of concave curvature, based on the observation – later confirmed psychophysically [Braunstein et al. 1989; DeWinter and Wagemans 2006] – that human-generated part boundaries tend to terminate at or near such minima. Based on this 2D Minima rule, several researchers have devised more complete systems to parse silhouettes using curvature minima [Singh et al. 1999; Siddiqi and Kimia 1995; Siddiqi et al. 1996]; but the 2D Min-

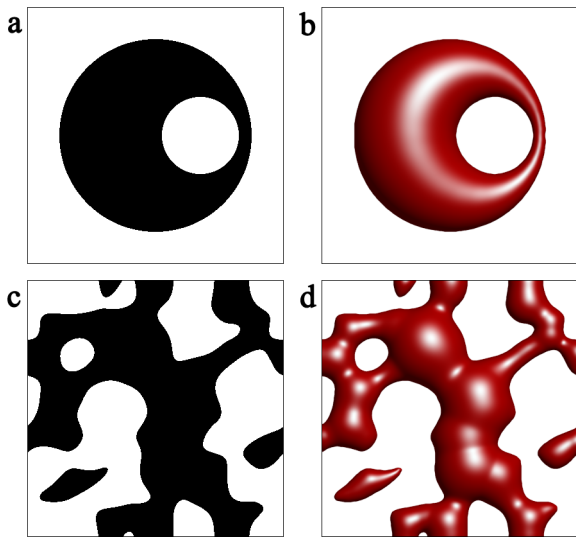


Figure 5: (a) An offset annulus. (b) The Puffball inflation of 5a. Both the wide and narrow bends of the resulting inflation have circular cross-section, demonstrating a deep level of inherent scale-invariance in Puffball inflation. (c) A complex, random mask achieved by thresholding low-pass noise. (d) Puffball successfully inflates the mask despite multiple separate components and the input extending outside the image domain.

ima Rule must be augmented by significant number of additional rules to generate consistently intuitive segmentations. Several have observed that medial axis structures can offer more robust insights into the perceptual structure of contours and silhouettes [Feldman and Singh 2006; Froyen et al. 2010].

Hoffman and Richards' 2D Minima Rule is derived from considerations of 3D shapes, that is, the part boundaries of a three-dimensional region are indicated by loci of minimal principal curvature on the surface of that region. This Three-Dimensional Minima rule is less ambiguous and more complete than the 2D Minima rule, and suggests an alternative application of the Minima rule to silhouette part segmentation. If one can map a silhouette to a smooth three-dimensional region, and locate the Minima-Rule-based boundaries on the surface of that region, one can project the resulting segments back into two dimensions to get a segmentation of the original silhouette. We find that a scale-invariant inflation like Puffball yields 3D shape information that supports intuitive segmentation.

Figure 6 depicts the Puffball segmentation process. First, the silhouette to be segmented is inflated using Puffball. According to the 3D Minima Rule, part boundaries are located along loci of minimal principal curvature, which are visibly evident in Figure 6b. However, rather than locating the full loci, a simpler approach is to only consider points *along the top* of the shape; more accurately, these are the points where the gradient in the direction of the most convex principal curvature is zero. Points of minimal principal curvature along the top of the shape consistently occur at the center of reasonable part boundaries (see Figure 6c). Extending these points to lines across the shape gives the Puffball-based part boundaries, which yield a perceptually intuitive segmentation of the silhouette (Figure 6d).

Figure 7 describes the advantages this approach confers over traditional 2D Minima Rule-based approaches. As shown in 7b, to segment both the index and middle finger from the palm, two part boundaries must terminate at the same curvature minimum, be-

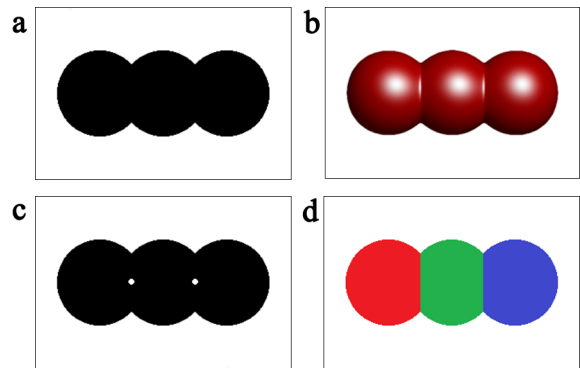


Figure 6: The Puffball segmentation process. (a) An initial silhouette. (b) The Puffball inflation. (c) Points of maximal principal curvature. (d) The resulting segmentation.

tween the two fingers. If only curvature minima are measured, however, this cannot be predicted, as it cannot be known whether two part-lines terminate at any given boundary. Also, any part boundary at the base of the index finger will have a curvature minimum at only one endpoint, making it even more difficult to identify. A 2D Minima rule-based approach offers no clear way to locate both boundaries. However, in the Puffball inflation of the shape, both boundaries are clearly distinguishable as zones of negative principal curvature (Figure 7c); hence, Puffball segmentation gives an intuitive result (Figure 7d). Further results are shown in Figure 8.

To evaluate this segmentation approach, a pilot experiment was run in which subjects on Amazon Mechanical Turk evaluated Puffball segmentations in comparison with two alternative algorithms. Puffball and our best effort implementations of the Necks and Limbs algorithm [Siddiqi and Kimia 1995] and the Shortcut Rule [Singh et al. 1999] were run on twenty-four silhouettes, eight each from three classical part segmentation categories: animals, hand tools, and human poses. Example segmentations of these stimuli are shown in Figure 9. In the experiment, the Mechanical Turk subject was presented with the original silhouette, as well as two seg-

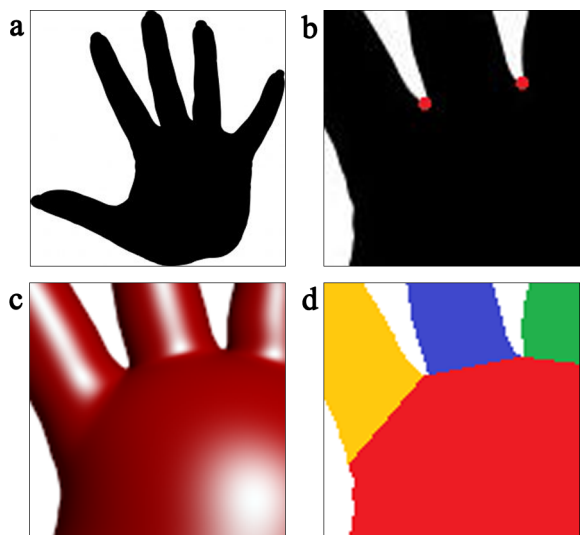


Figure 7: (a) A silhouette with a clear part structure. (b) The 2D Minima Rule is insufficient for these two boundaries. (c,d) Puffball segmentation yields the appropriate parsing.

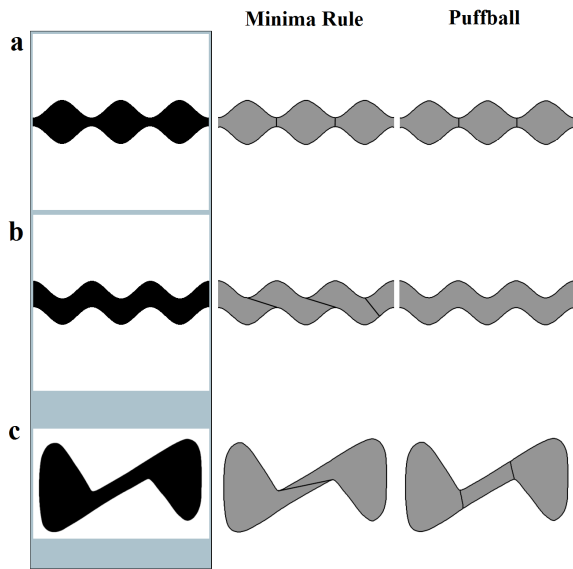


Figure 8: Contrasting the Minima rule and inflation based approaches. (a,b) As the curvatures of the contours of silhouettes (a) and (b) are identical, the Minima rule must either include part boundary endpoints in both silhouettes or neither. Regardless of how these endpoints are corresponded, they yield non-intuitive results. Inflation-based segmentation, however, evaluates these silhouettes very differently, as does our visual system. (c) A zig shape. Because a curvature minimum is present at either corner of the "zig", the simplest Minima rule-based part boundary is diagonally between them. But this seems incongruous the perceptual structure of the shape, which is much more similar to the part prediction made by our approach.

Puffball vs. Necks and Limbs			
	# Trials	Puffball Pref.	Proportion
Animals	320	222	0.694 (**)
Tools	320	195	0.609 (**)
Humans	320	218	0.681 (**)
Total	960	635	0.661
Puffball vs. The Shortcut Rule			
	# Trials	Puffball Pref.	Proportion
Animals	320	163	0.509
Tools	320	179	0.559 (*)
Humans	320	209	0.653 (**)
Total	960	551	0.574 (**)

Table 1: Proportion of trials in which Puffball segmentation was preferred over Necks and Limbs segmentation, and the Shortcut Rule. (*) indicates $p < 0.025$, (**) indicates $p < 0.001$.

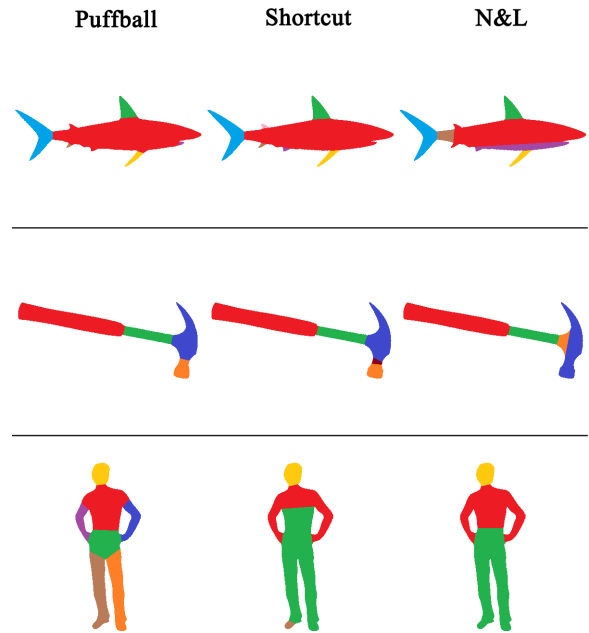


Figure 9: Part segmentation results on silhouettes from each of the three shape categories. Solid areas of color represent estimated parts. The human silhouette offers particular trouble to the 2D Minima Rule-based approaches, as both arms and legs are bounded by part boundaries with only one curvature minimum endpoint, much like the index finger in Figure 7. In addition, the boundaries of the legs share the same single minimum endpoint.

mentations (one of them Puffball segmentation); they were asked to choose the segmentation that looked more correct. This was done 40 times for each comparison, leading to a total of 960 comparisons (320 for each category) for each of the Necks and Limbs and the Shortcut rule. It is worth noting that the competing algorithms are our implementations of previous work, and thus likely do not represent the full potential of those algorithms or approaches.

Results of this experiment are shown in Table 1. As the table shows, Puffball segmentations were preferred well over both competing segmentations in every category except one. Overall, though the preferences were far from absolute, Puffball was selected a significantly higher percentage of the time; in most categories, this statistical significance was very pronounced. These results suggest that our segmentation approach, though it includes no explicit measurement of contour curvature and never locates contour minima, can perform as well as or better than more classical Minima-rule-based algorithms.

3.2 Image-Based Material Transfer

Another interesting problem is a variant of texture transfer. Consider the image of the strawberry in Figure 10a. Suppose we wanted to replicate the appearance of this strawberry on a novel shape, such as the donut in figure 10b. The naïve approach would require accurately extracting the three-dimensional geometry of both objects, separating the effects of global shading and local reflectance, determining the global statistics of the surface texture, replicating the source texture on the novel shape, and re-combining the reflectance and shading. A more desirable alternative would be one which requires no explicit knowledge of either three-dimensional shape, and operates entirely in the image domain.

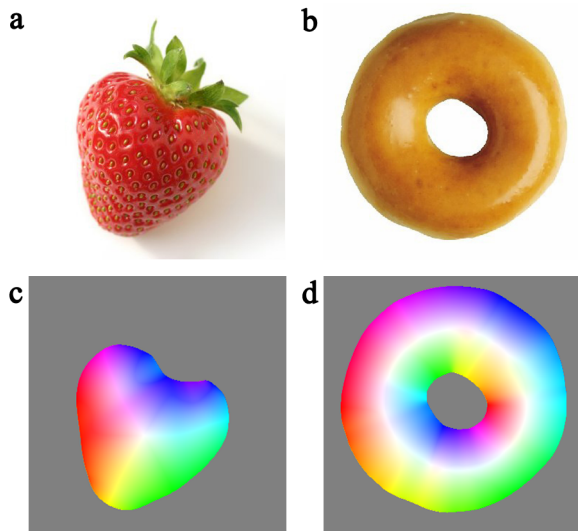


Figure 10: Image-based material transfer. (a,b) A source and target image. (c,d) The shape-based descriptor of interior points as determined by the Puffball surface normals. Here, saturation corresponds to how peripheral a point is, and hue represents the direction it lies away from the center.

If the rendered image is to appear accurate, the local image behavior at any pixel must be consistent with that of the source image. This problem was touched on briefly by Efros and Freeman [2001], but in the absence of any shape information, their technique could only be applied to surfaces under similar lighting conditions. In general, the local image behavior in an image of three-dimensional surface depends not only on the surface texture but on the shape of the object. What is needed is a representation of where an interior point lies relative to the shape. A smooth, scale-invariant inflation such as Puffball gives us this representation. If we take the surface normal of the inflation of a silhouette, that normal vector provides a smooth, robust representation of where every interior point lies within the shape (see Figures 10c and 10d): in the center, near the edge, or somewhere in between. With this representation, a target texture can be rendered while maintaining both local image consistency and consistency with the global structure of the shape.

With this measure in hand, we implemented a image-based material transfer algorithm inspired by the texture synthesis approach of Lefebvre and Hoppe [2005]. In brief, our approach synthesizes the novel image coarse-to-fine in a Gaussian pyramid, using a “Gaussian stack” of the source image as a basis. At each level, the algorithm constructs a coordinate image, in which each pixel of the target image refers to a location in the source image at the appropriate level of the Gaussian stack. This coordinate image is updated several times to ensure that for each pixel p in the target image, the source pixel q to which it refers has a similar image neighborhood and similar location relative to the shape (as determined by Puffball inflation). The coordinates are then upsampled to a finer scale and the process is repeated.

Figure 12 compares the results of our material transfer algorithm and that of Efros and Freeman [2001]. It is clear that the integration of shape information improves performance, especially when the lighting of the source and target shapes are very different. Nevertheless, the algorithm does not require explicit or accurate knowledge of the object’s *actual* shape; only the silhouette is required. Figure 11 shows further texture synthesis results. Even in circumstances when the inflated shape is missing much of the source object’s ac-

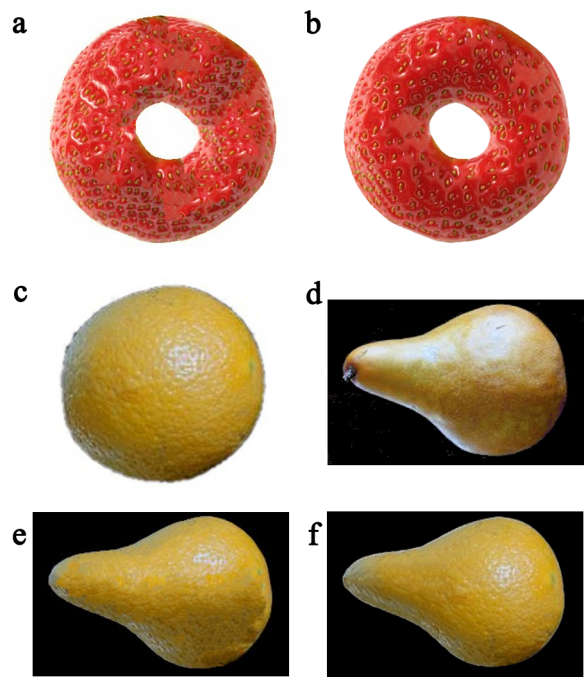


Figure 12: Comparison with Efros and Freeman [2001]. (a) The result of Efros and Freeman’s algorithm on the source and target image in Figure 10. (b) The results of Puffball material transfer on the same images. (c,d) A source and target image from Efros and Freeman [2001]. (e) Efros and Freeman’s result on images 12c and 12d. (f) Our results on images 12c and 12d.

tual geometry, as in the case of the rock image, a realistic-appearing surface texture can still be successfully produced.

4 Conclusion

We have shown how scale invariant inflation can be usefully applied to two very different image-based tasks: segmentation of silhouettes, and material transfer with 3D objects. We have also introduced a novel technique for scale invariant inflation, called Puffball. Puffball’s definition and implementation are extremely simple, and the results are intuitive and well-behaved. And many other problems can benefit from the application of scale-invariant inflation: lighting direction estimation, shape from shading, material analysis, grasping and navigation could all make use of such a tool.

Transformations between 2D and 3D imagery come up in many contexts, and a great many tools, some quite elaborate, have been developed to meet the needs of particular tasks. We do not claim that Puffball is the ideal solution for every task; nor do we doubt that it could be augmented in various ways to broaden its utility. However, in this paper we have resisted the temptation to add complexity so that we can explore Puffball in its simplest form.

We think of Puffball as analogous to the Sobel edge detector: not always the most sophisticated tool on the shelf, but one so simple and intuitive that every vision or graphics researcher should know it. We feel that it is a worthy addition to the basic toolbox of researchers in vision and graphics, where many more potential uses and applications undoubtedly wait to be uncovered.

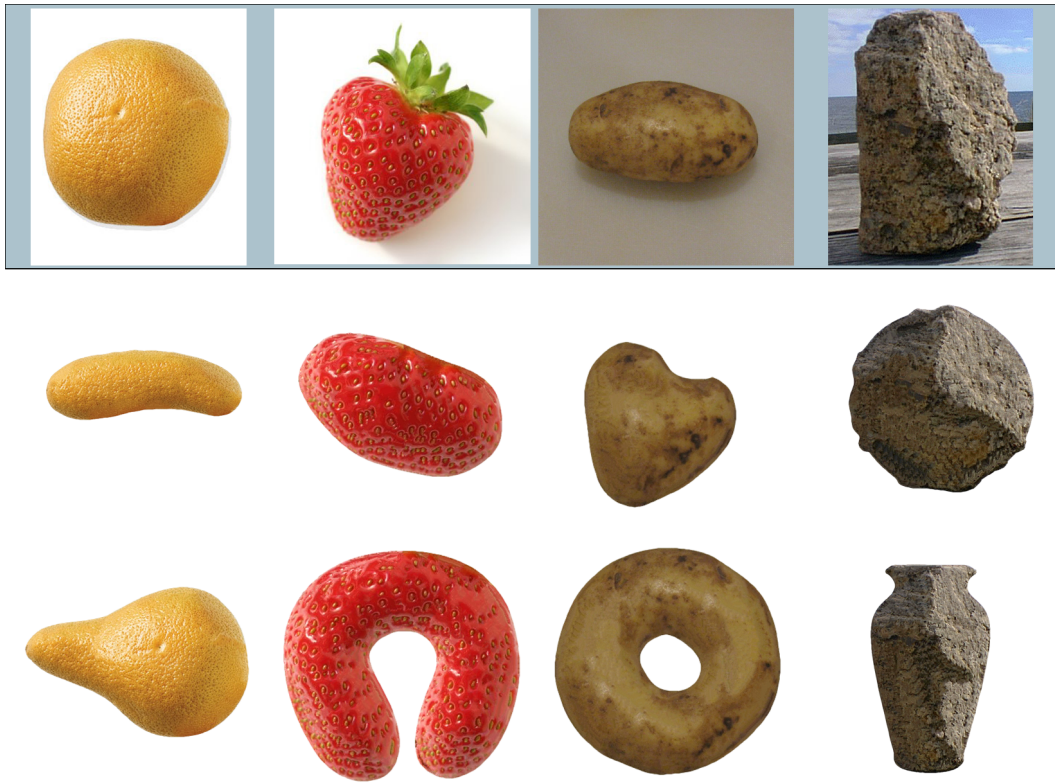


Figure 11: Additional material transfer results.

Acknowledgements

This research was supported by a Special Training Grant from the National Eye Institute.

References

- ALEXE, A., GAILDRAT, V., AND BARTHE, L. 2004. Interactive modelling from sketches using spherical implicit functions. In *International Conference on Computer Graphics, Virtual Reality, Visualisation and Interaction in Africa*.
- BLUM, H. 1967. A transformation for extracting new descriptors of shape. In *Models for the Perception of Speech and Visual Form*, W. Whalen-Dunn, Ed. MIT Press, 362–380.
- BRAUNSTEIN, M., HOFFMAN, D. D., AND SAIDPOUR, A. 1989. Parts of visual objects: An experimental test of the minima rule. *Perception* 18, 16, 817–826.
- DEWINTER, J., AND WAGEMANS, J. 2006. Segmentation of object outlines into parts: A large-scale integrative study. *Cognition* 99, 3, 275–325.
- EFROS, A. A., AND FREEMAN, W. T. 2001. Image quilting for texture synthesis and transfer. In *International Conference on Computer Graphics and Interactive Techniques*, 341–346.
- FELDMAN, J., AND SINGH, M. 2006. Bayesian estimation of the shape skeleton. *Proceedings of the National Academy of Sciences* 103, 47, 18014–18019.
- FROYEN, V., FELDMAN, J., AND SINGH, M. 2010. A bayesian framework for figure-ground interpretation. In *Advances in Neural Information Processing Systems*, vol. 23, 631–639.
- HOFFMAN, D. D., AND RICHARDS, W. 1987. Parts of recognition. In *Readings in computer vision: issues, problems, principles and paradigms*.
- IGARISHI, T., MATSUOKA, S., AND TANAKA, H. 1999. Teddy: a sketching interface for 3d freeform design. In *International Conference on Computer Graphics and Interactive Techniques: ACM SIGGRAPH Courses*.
- KARPENKO, O. A., AND HUGHES, J. F. 2006. Smoothsketch: 3d free-form shapes from complex sketches. *ACM Transactions on Graphics* 25, 3, 589–598.
- KARPENKO, O., HUGHES, J. F., AND RASKAR, R. 2002. Free-form sketching with variational implicit surfaces. *Computer Graphics Forum* 21, 3, 585–594.
- LEFEBVRE, S., AND HOPPE, H. 2005. Parallel controllable texture synthesis. *ACM Transactions on Graphics* 24, 3, 777–786.
- OSWALD, M. R., TOPPE, E., KOLEV, K., AND CREMERS, D. 2009. Non-parametric single view reconstruction of curved objects using convex optimization. In *Proceedings of the 31st DAGM Symposium on Pattern Recognition*, 171–180.
- PENTLAND, A. P. 1990. Automatic extraction of deformable part models. *International Journal of Computer Vision* 4, 2, 107–126.
- PRASAD, M., ZISSERMAN, A., AND FITZGIBBON, A. 2006. Single-view reconstruction of curved surfaces. In *Proceedings of 2006 IEEE Computer Society Conference on Computer Vision and Pattern Recognition*, 1345–1354.
- SIDDIQI, K., AND KIMIA, B. B. 1995. Parts of visual form: Computational aspects. *IEEE Transactions on Pattern Analysis and Machine Analysis* 17, 3, 239–251.

- SIDDIQI, K., TRESNESS, K. J., AND KIMI, B. B. 1996. Parts of visual form: Psychophysical aspects. *Perception* 25, 4, 399–424.
- SINGH, M., SEYRANIAN, G. D., AND HOFFMAN, D. D. 1999. Parsing silhouettes: the shortcut rule. *Perception and Psychophysics* 61, 4, 636–660.
- TAI, C.-L., ZHANG, H., AND FONG, C.-K. 2004. Prototype modeling from sketched silhouettes based on convolution surfaces. *Computer Graphics Forum* 23, 1, 71–83.
- TERZOPOULOS, D., WITKIN, A., AND KASS, M. 1987. Symmetry-seeking models and 3d object recognition. *International Journal of Computer Vision* 1, 3, 211–221.
- TERZOPOULUS, D., AND WITKIN, A. 1988. Physically based models with rigid and deformable components. *IEEE Computer Graphics and Applications* 8, 6, 41–51.
- TSE, P. U. 2002. A contour propagation approach to surface filling-in and volume formation. *Psychological Review* 109, 1, 91–115.
- ZHANG, L., DUGAS-PHOCION, G., SAMSON, J.-S., AND SEITZ, S. M. 2002. Single-view modeling of free-form scenes. *The Journal of Visualization and Computer Animation* 13, 4, 225–235.